Electrostatic mechanism of strong enhancement of light emitted by semiconductor quantum wells

A. Llopis, J. Lin, S. M. S. Pereira, T. Trindade, M. A. Martins, I. M. Watson, A. A. Krokhin, and A. Neogi

Phys. Rev. B **87**, 201304 — Published 30 May 2013

DOI: 10.1103/PhysRevB.87.201304

Electrostatic mechanism of strong enhancement of light emitted by semiconductor quantum wells

A. Llopis,[1] J. Lin,[1] S.M.S. Pereira,[2] T. Trinidade,[2] M.A. Martins,[2] I.M. Watson,[3] A.A. Krokhin,[1,*] and A. Neogi[1]

[1] *Department of Physics, University of North Texas, P.O. Box 311427, Denton, TX 76203*
[2] *CICECO, University of Aveiro, 3810-193 Aveiro, Portugal*
[3] *Institute of Photonics, University of Strathclyde, Glasgow, G4 0NW, UK*

(Dated: April 8, 2013)

Currently, it is considered that the carrier recombination rate in semiconductors can be modified by metals due to pure electrodynamic interactions through surface plasmons. We propose here an electrostatic mechanism for carrier-metallic nanoparticle interaction comparable in effect to plasmonic interactions. Arising from Coulomb attraction of electrons and holes to their images in metal, this mechanism produces large carrier concentrations near metallic nanoparticle. Increased concentration results in increased quantum efficiency and enhance the rate of e-h recombination. This manifests as emission enhancement in InGaN quantum wells radiating in the Near-UV region. The proposed fundamental mechanism provides a new perspective for improving the efficiency of broad-band light emitters.

PACS numbers: 78.55.-m, 78.67.Pt, 82.53.Mj

The internal quantum efficiency (IQE) of semiconductor light emitters depends primarily on the radiative electron-hole recombination rate, which can be significantly modified by electromagnetic coupling of the carriers to surface plasmon (SP) modes. This electrodynamic interaction shows promise for applications from light emitters to communications[1–6]. Essential enhancement of light emission has been demonstrated in various systems, including a semiconductor quantum well (QW) , a[1–3] distributed Bragg reflector[7], an ionized center in a diamond[8], and a plasmonic nanocavity[9]. This enhancement is due to interaction of the carriers with the field of surface plasmons (SP). If the frequency of emitted light matches the resonant frequency of the SPs, the rate of spontaneous e-h recombination increases by up to two orders of magnitude due to Purcell effect [10]. Metallic nanoparticles may also enhance photocurrent generated in a semiconductor diode [11] and light-absorbing chlorophyll molecules [12] providing resonant electromagnetic coupling between the metal and light.

Carriers in the QW, however, interact with the metal not only through the SP fields but also through Coulomb forces. Coulomb attraction of the carriers to a neutral metallic nanoparticle (NP) increases the local concentration of e-h pairs, leading to efficient recombination and a strong enhancement in photoluminescence (PL). This universal (i.e. independent of the type of metal) electrostatic mechanism is not restricted by the frequency matching conditions. Here we present a comprehensive model for, and experimental evidence of an electrostatic mechanism for enhancement of light emission in InGaN/GaN QW. The proposed theory correctly predicts several significant new features which are related to the electrostatic nature of the mechanism: strongly inhomogeneous light emission with high concentration near the NPs, saturation with increasing pumping power and an anomalously long decay time observed in time-resolved PL experiments. We have ruled out the plasmonic mechanism in our experiments since the energy of SP resonance at the metal-semiconductor interface $\hbar\omega_s = 2.3$ eV is well below the energy of the light emitted from the QW $\hbar\omega = 3.05$ eV.

It is well-known that depending on the final density of photonic states, the environment may either suppress[13] or enhance[1,2,9,10,14] the spontaneous emission rate. Much less attention has been paid to local modulation of carrier concentration. The concentration of e-h pairs depends on the excitation power and is usually homogeneous over the QW. In the case of an inhomogeneous distribution, the regions with increased concentration have higher emission intensity leading to localized emission peaks. The probability of radiative Γ_r and nonradiative Γ_{nr} recombination both depend on the concentration n of e-h pairs. However, it is known that the nonradiative component is linear in n, $\Gamma_{nr} = An$, whereas the radiative component is quadratic in n, $\Gamma_r = Bn^2$. Therefore, the internal quantum efficiency (IQE)

$$\eta = Bn^2/(An + Bn^2) \tag{1}$$

increases with concentration of carriers[15]. Here we have neglected the cubic Auger recombination which becomes significant at much higher concentrations.

Therefore modulating the concentration of carriers in a QW may increase IQE and localize the emission – a problem which so far has only been considered for plasmonic devices[16,17]. To generate this inhomogeneous distribution we have placed metallic NPs within a QW, Fig. 1. Neutral metal attracts electrons and holes, causing the carriers to drift towards, and concentrate near, the NP. The size of the NP plays a principal role here, determining the increase in concentration and light intensity. The drift is not destroyed by thermal fluctuations if the ratio $\gamma = (e^2/\varepsilon R)/kT \sim 1$. For the effect to be observable at 300K, this condition requires that the typical size R of the NP be $R < 50$ nm given that $\varepsilon \sim 10$.

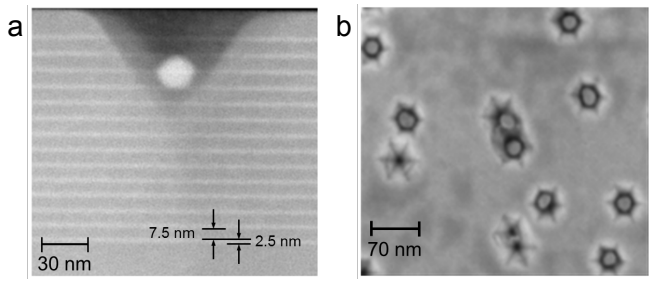

FIG. 1: Images of the heterostructure. (a) TEM of the InGaN multi-QW showing a gold NP embedded within the naturally occurring pit. (b) SEM of the same structure.

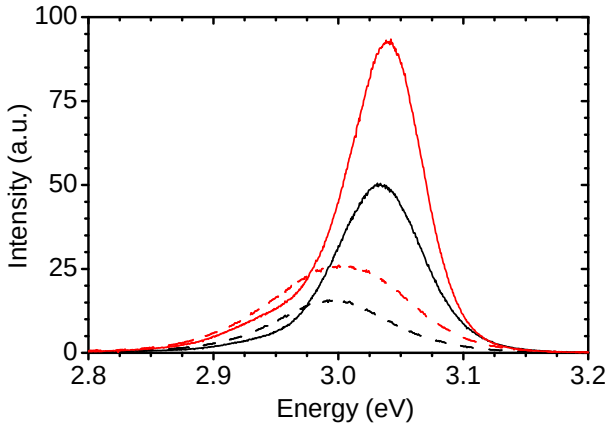

FIG. 2: Color online. Enhanced PL emission in Au/InGaN multi-QW. Spectra from the reference (black) and gold NP InGaN QWs (red). Enhancement is observed in the near-UV region for the sample with gold NPs. At $T = 77$K (solid) the effect of enhancement is noticeably stronger than at $T = 300$K (dashed). A blue-shift in the spectra on the order of 10 meV is present at both temperatures.

We measured the PL enhancement from the same material heterostructures of InGaN/GaN which were previously used in Ref.[2] to demonstrate the plasmonic mechanism of enhancement[18]. We, however, used gold instead of silver in order to exclude resonant coupling to SPs and also formation of hybrid excitons[19]. The positions and geometry of the metallic NPs are pictured in Fig. 1. NPs of typical size of $R \approx 17$nm are embedded in inverted hexagonal pits at the surface resulting from threading dislocations[20]. As shown in Fig. 1, this peculiar feature of InGaN-multi-QW growth provides an elegant means of incorporating the metallic NPs directly into the core of the heterostructure without any strain modification[21].

The PL spectra of the multi-QW with and without gold NPs are shown in Fig. 2 with a maximum PL intensity at $\hbar\omega = 3.05$ eV. There is roughly a 60% enhancement in the PL emission with gold at room temperature increasing to 80% enhancement at 77K. As mentioned before, a gold thin-film (or a gold NP) does not enhance the emission of an InGaN QW due to having a lower SP energy. Light scattering by the gold NPs with $R < 50$ nm also cannot have any significant effect at $\hbar\omega = 3.05$ eV. Scattering cannot be a source of enhancement also because of the 10 meV blue shift in the spectrum. Thus, we may completely rule out light scattering along with plasmonic enhancement and other known mechanisms as a source of the enhancement presented in Fig. 2. The known non-resonant plasmonic mechanisms[22] are ruled out since they require special geometry.

Instead, the Coulomb attraction of the free carriers to their image charges acts as a catalyst for recombination by increasing the local concentration of carriers and leading, according to Eq. (1), to higher IQE. Image charges, cause both electrons and holes to drift towards the NP. Since the accumulation of e-h pairs occurs near NPs, the enhancement of intensity is strongly inhomogeneous, $\eta = \eta(\mathbf{r})$. Fig. 2 shows average over the sample intensity measured in the far-field. Although the total number of electron transitions is fixed by the number of available e-h pairs in the QW, the regions with higher concentration have higher ratio Γ_r/Γ_{nr} resulting in higher IQE.

The origin of this electrostatic mechanism is best demonstrated by Thomson's theorem which states that a neutral conductor attracts *any* given set of electric charges[23]. Therefore electrons and holes are attracted towards the metal NPs. They are attracted even if they form excitons. A direct manifestation of this attraction is stronger enhancement at 77K than at 300K shown in Fig. 2. The attraction of a single carrier located at a distance r from a metallic sphere of radius R decays fast far away from the sphere, $eE(r) \sim r^{-5}$. However, close to the surface, it grows as $eE(r) \sim (r-R)^{-2}$. This Coulomb force leads to a permanent drift of the carriers. The local concentrations of carriers are obtained from the coupled non-linear diffusion equations in the presence of the electrostatic force $e\mathbf{E}(\mathbf{r})$. For electrons it has the following form:

$$\dot{n}_e = D_e \nabla^2 n_e + \frac{eD_e}{kT} \nabla \cdot (\mathbf{E} n_e) - n_e(A - Bn_h) + g. \quad (2)$$

The equation for holes is obtained by replacement $e \Leftrightarrow h$. Here $D_{e,h}$ are the diffusion coefficients, and g is the density of e-h pairs produced by the pumping laser per second. The field $\mathbf{E}$ in the drift term is obtained from the Poisson equation:

$$\nabla \cdot (\varepsilon \mathbf{E}) = 4\pi \left[e(n_h - n_e) + e'\delta(\mathbf{r} - \mathbf{r}') - e'\delta(\mathbf{r}) \right], \quad (3)$$

where the charge density has three components. The first is the standard non-compensated bulk charge. Second is the image charge $e' = -eR/r$ induced by a carrier e in the QW. This image charge is situated inside the nanosphere at a distance $r' = R^2/r$ from its center. Third is a charge $-e'$ at the center which provides electrical neutrality.

The increased intensity in Fig. 2 for $T = 77K$ is partially related to a natural increase of the probability of

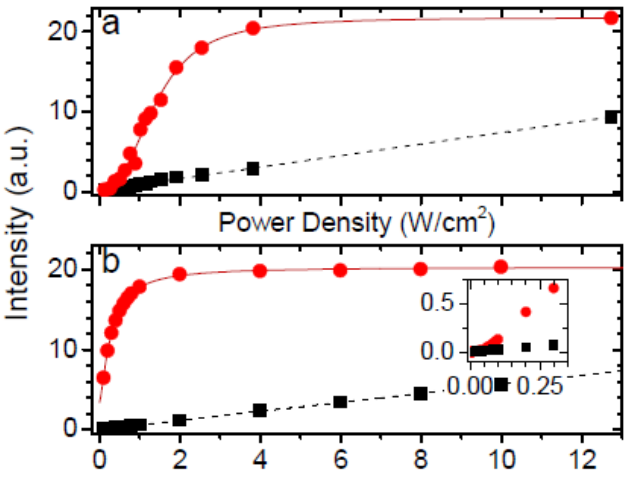

FIG. 3: Color online. (a) Power dependent PL intensity for the Au/InGaN (red circles) and reference systems (black squares). (b) Simulated intensity $I \propto \int n_e n_h d\mathbf{r}$ versus pump power for the Au/InGaN and reference systems. The concentrations are obtained numerically as stationary solutions of Eqs. (2) and (3). The inset shows effect of the depletion layer at low powers.

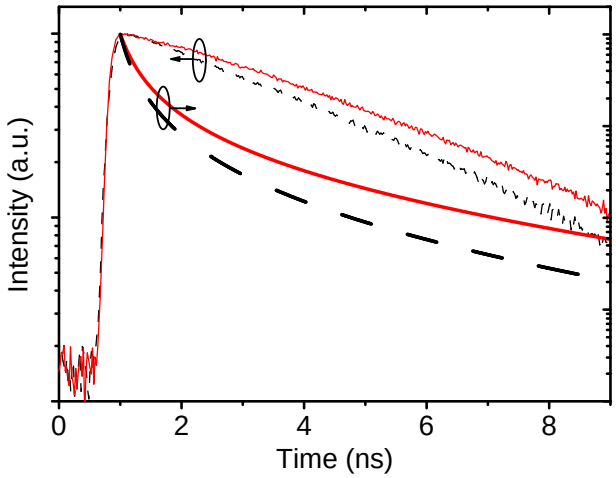

FIG. 4: Color online. Time-dependent photoluminescence for the QW with (solid, red) and without (dashed, black) nanoparticles. Left vertical axis: Measured time-dependent PL. Right vertical axis: Numerical simulation of the time evolution of intensity derived from Eq. (2) using material parameters from the InGaN system. The excitation modeled as an instantaneous gaussian laser pulse at $t = 0.5$ ns. Note that the simulation qualitatively reproduces the apparent increase in decay lifetime observed experimentally. The simulation diverges from the experimental results due to neglect of Debye screening and the Stark effect.

radiative recombination at lower temperatures. If this were the only reason, however, the enhancement would be identical to that in the reference sample, which is not the case. Stronger enhancement in Fig. 2a is due to $1/T$ dependence of the drift term in Eq. (2). Physically this means that the width of the region $\gamma R \propto 1/T$ where drift is not destroyed by thermal fluctuations increases at lower temperatures.

The proposed mechanism explains the enhanced spectra in Fig. 2. At the same time the emission spectrum of the QW coated by gold film does not exhibit enhancement at all[1–3]. In this case the carriers in the QW are also attracted towards their images. However, in the plane geometry electrons and holes drift towards the metal film, without changing the average in-plane separation between them. It turns out that the increase of the concentration only along a single coordinate is not sufficient to produce the effect of enhancement. In this case normal to the metal forces may only reduce the effective width of the QW. This gives rise to the blue shift which was reported in Refs.[1–3] but not explained so far. Gold nanospheres, being practically point attractors, lead to both effects – blue shift and emission enhancement. The image-charge-induced blue shift has been observed previously in the case of dielectric-dielectric interfaces[24].

The electrostatic mechanism exhibits a specific power dependence. Fig. 3 shows how the enhancement saturates as pump power is increased. The source of this power dependence is competition between the Debye screening of the image charges by carriers and the increased IQE as the carrier concentration increases (see Eq. (1)). The general form of saturation is correctly predicted in our simulation results in Fig. 3b. We also note at this point that, although the calculated intensity in Fig. 3 exhibits the correct saturation at powers > 4 W/cm^2, the model based on Eqs. (2) and (3) fails to predict the change of curvature in the experimental data in Fig. 3a at low power (< 1W/cm^2). This obvious "retardation" in saturation is due to the formation of a 40 nm wide depletion layer in the InGaN along the area of contact with the gold NP. By calculating the depletion layer we are able to include the band-bending effects in the electric field in Eq. (3). When this corrected field is introduced, we find that a flex point appears in the curve, as shown in the inset in Fig. 3b.

A principal difference in origin of plasmonic and electrostatic enhancement can be seen in the time-resolved PL measurements in Fig. 4. Plasmonic enhancement is accompanied by a strong decrease in the decay lifetime[1,2,25]. Contrary to this, our samples with metal NPs show (see Fig. 4) an increase in the decay constant α ($I(t) \propto \exp(-\alpha t)$)which in our case is not the same as the inverse decay lifetime $\Gamma_r + \Gamma_{nr}$. The two are equal, if the carriers recombine near the point where they are generated. This scenario is realized when the drift of the carriers is absent, i.e. the enhancement is due to the plasmonic mechanism.

Contrary to the plasmonic increase of the decay constant α , our samples with metal NPs show that α decreases. The origin of this decrease is related to the electrostatic drift and inhomogeneous distribution of carriers in the QW. Each NP is surrounded by a narrow

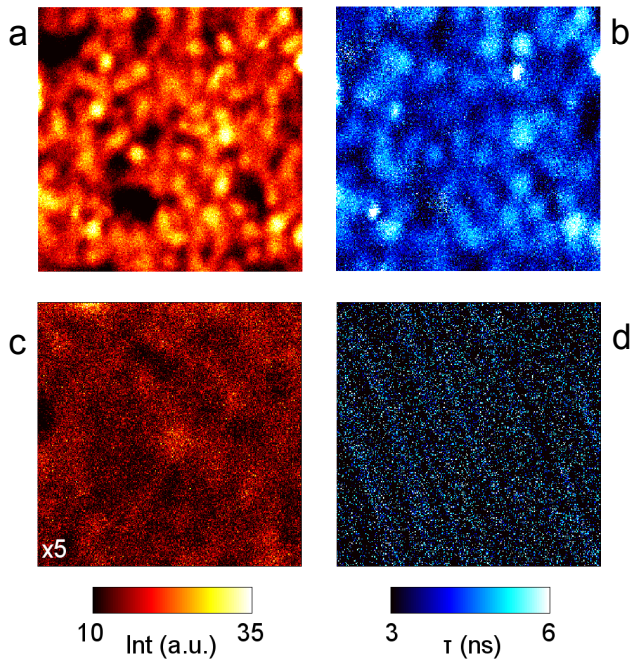

FIG. 5: (a) Time-resolved PL intensity of the measured over a 10 × 10 μm region of the QW. (b) Decay lifetime of the same region. (c) Reference system PL intensity over a 10 × 10 μm region. (d) Decay lifetime for the reference system. Note the difference in scale of the inhomogeneity and how a correlation between intensity and lifetime is only present in the Au/InGaN system. Specifically the brighter regions are correlated with longer PL lifetimes.

layer of width $\sim \gamma R$ where the recombination rates and the IQEs are higher than in the rest of the QW. While in these layers the e-h pairs recombine much faster, the non-equilibrium carriers are not exhausted there due to permanent diffusive flow from the bulk of the QW. Each carrier drifting towards metallic NP increases its probability to recombine radiatevely. The probability of non-radiative recombination also increases but slower than the probability of radiative recombination. The further the carrier is situated from the NP the longer time it drifts before this probability is realized. Thus, the decay constant α deceases in the presence of metallic NP but in the case of electrostatic mechanism this decrease cannot be attributed to decrease of the recombination rate. The experimentally measured PL decay follows the time dependence which can be obtained from the intensity $I(t) \propto \int n_e n_h d\mathbf{r}$. Here the concentrations are the time-dependent solutions of Eqs. (2) and (3) where the pumped density $g \propto \delta(t)$ is the initial concentration of e-h pairs produced by the femtosecond pulse. Numerical curve in Fig. 4 qualitatively reproduces experimentally observed increase of the PL decay. The observed intensity enhancement and longer PL decay time occur due to those e-h pairs which would decay non-radiatevely if there would be no gold NPs.

Strongly inhomogeneous distribution of emitted light over the surface of the sample is shown in fluorescence lifetime imaging in Fig. 5. There is significant change in inhomogeneity of photoemission between the reference and Au NP samples. Also the Au NP sample exhibits a strong correlation between intensity and recombination lifetime, as predicted by the proposed model. This correlation is, however, entirely absent in the reference sample. Anomalous increase of the decay constant has been recently observed in the experiment with Tamm plasmons[7]. Most likely this anomaly is due to electrostatic interaction of the excitons in GaAs QW with gold microdisk.

While both plasmonics and the electrostatic mechanisms have a similar end result – enhancement – they have different physical origins. Because of their similarity it is important to point out the following: Firstly, it may be possible to tailor systems whereby *both* mechanisms are simultaneously manifested to further increase the efficiency of light-emitting devices. Recently, anomalously large enhancements have been reported in In/InN[26], and Ag/ZnO systems[27]. Since the geometry in these systems is favorable to strong electrostatic interaction, we believe that this anomalously large increase in enhancement may be attributed to the simultaneous manifestation of these two mechanisms. Secondly, it is possible that some effects currently attributed to plasmonics might instead arise from electrostatics. For example, the plasmonic mechanism has been invoked to explain enhancement in the emission of ZnO due to gold NPs[28] as well as emission in Si using silver NPs[29]. Since in these cases the emitted light does not match the corresponding resonant frequency, plasmonic enhancement should be ruled out.

In conclusion, the results here clearly illustrate the existence of a universal non-resonant mechanism for enhancement of carrier recombination arising from the interaction of carriers with their image charges within a metallic NP. The hallmarks of this effect are increased carrier concentration resulting in highly localized light emission, increased IQE and decay PL constant, and saturation at high pump power. The image charge effect provides a means for enhancing optical emission in systems where the precise tailoring required by resonant plasmonic enhancement is not possible.

I. ACKNOWLEDGEMENT

The authors would like to acknowledge the support of the Center for Commercialization of Fluorescence Technologies (CCFT) at the University of North Texas Health Science in Fort Worth, Texas. The authors acknowledge the assistance of Dr. Ryan Rich and Dr. Zygmunt Gryczynski for the micro-photoluminescence measurements. This work is supported by the US Department of Energy grant # DE-FG02-06ER46312, NSF Grant # DMR-0520550, NSF IRES program # 623642, and by Fundação para a Ciência e Tecnologia (FTC/FEDER)

Project PTDC/CTM/101453/2008.

---

* Electronic address: arkady@unt.edu

[1] N.E. Hecker, R.A. Höpfel, N. Sawaki, Physica E **2**, 98 (1998); N.E. Hecker, R.A. Höpfel, N. Sawaki, T. Maier, and G. Strasser, Appl. Phys. Lett. **75**, 1577 (1999).

[2] A. Neogi, C.W. Lee, H.O. Everitt, T. Kuroda, A. Tackeuchi, E. Yablonovitch, Phys. Rev. B **66**, 153305 (2002).

[3] K. Okamoto, I. Niki, A. Shvartser, Y. Narukawa, T. Mukai, and A. Scherer, Nature Mat. **3**, 601 (2004).

[4] B. Fluegel, A. Mascarenhas, D.W. Snoke, L.N. Pfeiffer, and K. West, Nature Photon. **1**, 701 (2007).

[5] S. Maier, Nature Phys. **3**, 301 (2007).

[6] D.K. Gramotnev, and S.I. Bozhevolnyi, Nature Photon. **4**, 83 (2010).

[7] O. Gazzano, S. Michaelis de Vasconcellos, K. Gauthron, C. Symonds, J. Bloch, P. Voisin, J. Bellessa, A. Lemaître, and P. Senellart, Phys. Rev. Lett. **107**, 247402 (2011).

[8] J.T. Choy, B.J.M. Hausmann, T.M. Babinec, I. Bulu, M. Khan, P. Maletinsky, A. Yacoby, and M. Loncar, Nature Photon. **5**, 738 (2011).

[9] K. J. Russell, T.-L. Liu, S. Cui, and E. L. Hu, Nature Photon. **6**, 459 (2012).

[10] E.M. Purcell, Phys. Rev. **69**, 681 (1946).

[11] S.P. Sundararajan, K.G. Grady, N. Mirin, N.J. Halas, Nano Lett. **8**, 624 (2008).

[12] A.O. Govorov, I. Carmeli, Nano Lett. **7**, 620 (2007).

[13] S. Noda, M. Fujita, and T. Asano, Nature Photon. **1**, 449 (2007).

[14] J. Eschner, Ch. Raab, F. Schmidt-Kaler, and R. Blatt, Nature **413**, 495 (2001).

[15] Q. Dai, M.F. Schubert, M.H. Kim, J.K. Kim, E.F. Schubert, D.D. Koleske, M.H. Crawford, S.R. Lee, A.J. Fischer, G. Thaler, and M.A. Banas, Appl. Phys. Lett. **94**, 111109 (2009).

[16] J.A. Schuller, E.S. Barnard, W. Cai, C.Y. Jul, J.S. White and M.L. Brongersma, Nature Mater. **9**, 193 (2010).

[17] Y.C. Jun, K.C.Y. Huang, and M.L. Brongersma, Nature Comm. **2**, 283 (2011).

[18] More details about prepararion of the samples and optical measurements are given in Supplimental Information.

[19] W. Zhang, A.O. Govorov, and G.W. Bryant, Phys. Rev. Lett. **97**, 146804 (2006).

[20] Y. Chen, T. Takeuchi, H. Amano, I. Akasaki, N. Yamano, Y. Kaneko, S.Y. Wang, Appl. Phys. Lett. **72**, 710 (1998).

[21] S. Pereira, M.A. Martins, T. Trinidade, I.M. Watson, D. Zhu, C.J. Humphreys, Adv. Mater. **20**, 1038 (2008).

[22] D. E. Chang, A. S. Sorensen, P. R. Hemmer, and M. D. Lukin, Phys. Rev. Lett. **97**, 053002 (2006); L. Novotny and S.J. Stranick, Annu. Rev. Phys. Chem. **57**, 303 (2006); A. V. Akimov *et al.*, Nature (London) **450**, 402 (2007); Y. C. Jun, R. D. Kekatpure, J. S. White, and M. L. Brongersma, Phys. Rev. B **78**, 153111 (2008).

[23] L.D. Landau, E.M. Lifshitz, and L.P. Pitayevskii, *Electrodynamics of Continuous Media*, 2nd Ed., (Pergamon Press, Oxford, 1984).

[24] D.B. Tran Thoai, R. Zimmermann, M. Grundmann, and D. Bimberg; K. Tanaka, T. Takahashi, T. Kondo, T. Umebayashi, K. Asai, and K. Ema, Phys. Rev. B **71**, 045312 (2005); F. Rajadell, J.L. Movilla, M. Royo, and J. Planelles, Phys. Rev. B **76**, 115312 (2007).

[25] I. Gontijo, M. Boroditsky, E. Yablonovitch, S. Keller, U. K. Mishra, and S. P. DenBaars, Phys. Rev. B **60**, 11564 (1999).

[26] T.V. Shubina, A.A. Toropov, V.N. Jmerik, D.I. Kuritsyn, L.V. Gavrilenko, Z.F. Krasil'nik, T. Araki, Y. Nanishi, B. Gil, A.O. Govorov, and S.V. Ivanov, Phys. Rev. B **82**, 073304 (2010).

[27] J.B. You, X.W. Zhang, Y.M. Fan, Z.G. Yin, P.F. Cai, and N.F. Chen, J. Phys. D: Appl. Phys. **41**, 20 (2008).

[28] T. Chen, G.Z. Xing, Z. Zhang, H.Y. Chen, and T. Wu, Nanotechnology **19**, 43 (2008).

[29] S. Pilai, K. R. Catchpole, T. Trupke, G. Zhang, J. Zhao, and M. A. Green, Appl. Phys. Lett. **88**, 161102 (2006).